

# Electric-Field-Induced Lock-and-Key Interactions between Colloidal Spheres and Bowls

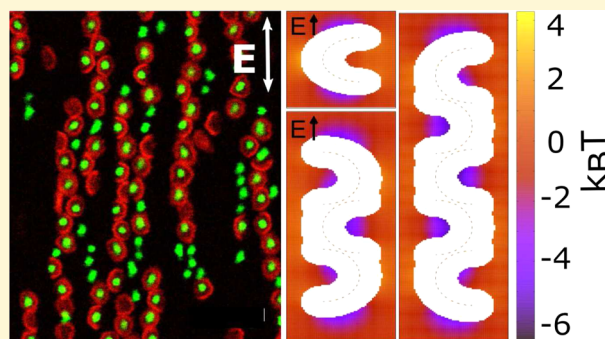
Marlous Kamp,<sup>\*,†,‡</sup> Nina A. Elbers,<sup>†,‡</sup> Thomas Troppenz,<sup>†,§</sup> Arnout Imhof,<sup>‡</sup> Marjolein Dijkstra,<sup>‡</sup> René van Roij,<sup>§</sup> and Alfons van Blaaderen<sup>\*,‡</sup>

<sup>‡</sup>Soft Condensed Matter, Debye Institute for Nanomaterials Science, Utrecht University, Princetonplein 1, 3584 CC Utrecht, The Netherlands

<sup>§</sup>Institute for Theoretical Physics, Utrecht University, Leuvenlaan 4, 3584 CE Utrecht, The Netherlands

**S** Supporting Information

**ABSTRACT:** To realize new and directed self-assembly (SA) pathways, the focus in colloid science and nanoscience has shifted from spherical particles and interactions to increasingly more complex shapes and interparticle potentials. This field is fueled by recent breakthroughs in particle synthesis, such as particles with complementary shapes that allow for specific lock-and-key interactions induced by depletants. Here, we show that electric fields form an alternative route for directing the SA of convex and concave colloids, with the additional advantage that the system now becomes switchable by external conditions. Both experimental and theoretical results are presented that validate the electric-field-induced assembly mechanism and show that even irreversibly bound composites can be generated by tuning the force balance. The successful isolation of the irreversible composite particles, in combination with generalization to different materials, shows that the current mechanism provides a versatile new path not only toward complex-particle synthesis but also toward directed self-assembly.



## INTRODUCTION

In the field of colloidal self-assembly, the focus in recent studies has shifted from spherical particles to anisotropic or more complex shaped particles and from spherical interaction potentials to more complex interactions. This shift in perspective is driven by newly invented synthesis routes that result in particles with complex shapes.<sup>1–3</sup> Examples include bowl-shaped particles,<sup>4</sup> flattened particles,<sup>5</sup> rods,<sup>6,7</sup> (hollow) cubes,<sup>8</sup> ellipsoids,<sup>9</sup> peanut-shaped particles,<sup>10</sup> platelets,<sup>11</sup> colloidal molecules,<sup>12–14</sup> colloidal clusters,<sup>15</sup> dumbbells,<sup>16,17</sup> and polyhedral particles.<sup>18</sup> Combining complex-particle shapes with anisotropic interactions opens many new avenues to manipulate self-assembly and materials properties. An example is the lock-and-key interaction between complementary-shaped particles<sup>19</sup> induced by depletants.<sup>20,21</sup> Depletion-induced interactions, driven by nonadsorbing polymers or particles (“depletants”), have an interaction range that is set by the size of the depletant, while the interaction energy is set by the concentration of depletants.<sup>22</sup> This allows for an independent tuning of the range and strength of depletion interactions.

Another way to induce inhomogeneous interactions is by means of external electric fields. Experimental approaches in this direction have already been described in literature.<sup>3</sup> For example, it is well-established that electric fields can be used to manipulate the orientation of colloidal particles. For silica rods, the alignment of the axis in the direction of an external electric

field can result in improved millimeter-ranged order in smectic phases<sup>23</sup> as well as in a transition from a plastic crystal or plastic glass to a crystal phase.<sup>24</sup> Such field alignment was also used to tailor the properties of films prepared from colloidal ellipsoids.<sup>25</sup> In addition, an electric field can be used to alter the structural behavior of the particles. As a result of the interaction of the induced polarizations, particles (spheres, rods, bowls, and other anisotropic shapes) can form long chains along the direction of an external electric field.<sup>23,26–29</sup> The behavior of mixtures of polarizable colloids of different geometric shapes is less well studied, although beautiful structures in the analogous case of magnetic particles and fields are known.<sup>30</sup> In principle the external field gives rise to a many-body problem, with couplings between the induced dipoles in both particle species that require self-consistent or recursive techniques<sup>31</sup> to calculate the polarization of the particles and the interactions between the particles. Insight can be gained from theoretical and computational studies,<sup>32–34</sup> and various methods have been developed in recent years to describe or predict field-induced alignment and interactions (e.g., the coupled dipole method<sup>3,35,36</sup>).

Received: October 27, 2015

Revised: January 20, 2016

Published: January 21, 2016

**Table 1. Composition of the Various Bowl–Sphere Mixtures in Water<sup>a</sup>**

sample	SiO <sub>2</sub> spheres (% (v/v))	PS spheres (% (v/v))	bowls (% (v/v))	salt (NaCl) (mM)	D <sub>2</sub> O (% (v/v))
SiO <sub>2</sub> -w4.5-1	51	0	22	4.5	0
SiO <sub>2</sub> -w8.3	38	0	38	8.3	0
SiO <sub>2</sub> -w4.5-2	5	0	81	4.5	0
PS-w4.5	0	70	16	4.5	0
PS-d3.8	0	23	9	3.8	57

<sup>a</sup>Mixtures were obtained by combining the stock dispersions in various ratios (see SI): the volume fractions (% (v/v)) indicated are fractions of the stock dispersions in the final mixture. The sample name reflects the sample composition: SiO<sub>2</sub> for silica spheres, PS for polystyrene spheres, “w” for pure water as a solvent, and “d” for D<sub>2</sub>O added as a solvent. The number indicates the salt concentration in millimolar. Any extra number (–1 or –2) was added to the name if samples with the same constituents were prepared at various bowl–sphere number ratios.

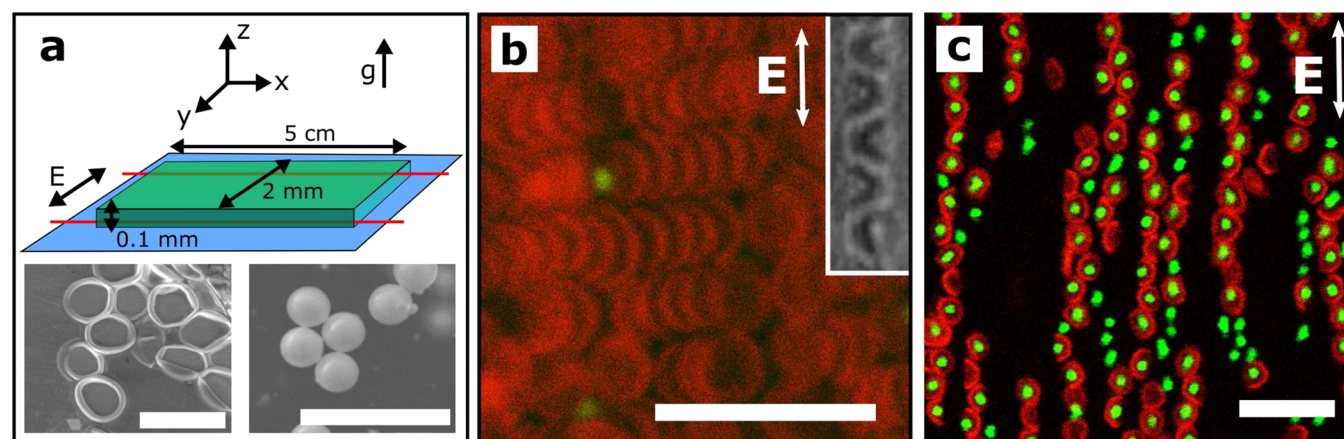


**Figure 1.** Electric-field-induced self-assembly. (a) Schematic drawing of the experimental setup used to create electric-field-induced lock-and-key interactions. The direction of the electric field ( $E$ ), the direction of gravity ( $g$ ), and the three spatial dimensions  $x$ ,  $y$ , and  $z$  (chosen along the length ( $x$ ), width ( $y$ ), and depth ( $z$ ) of the capillary) are indicated. Note that we used an alternating electric field with a frequency higher than the relaxation rate of a double layer (1 MHz). Scanning electron micrographs of bowl-shaped particles (left) and silica spheres (right) are shown in the inset. (b) Confocal micrograph of a sample region with a high concentration of bowls (RITC dyed, red). Bowls form stacks in a direction perpendicular to the electric field (19.1 V/mm, 30 mM NaCl). Note the alternating orientation of the bowls in a string. Inset: optical micrograph of a single chain of bowls. Note that in this optical image the bowls are the black objects. (c) Confocal micrograph of bowls and spheres self-assembled in an electric field. This image was taken of sample SiO<sub>2</sub>-w4.5-1 (see Table 1). Bowls (2.6  $\mu$ m diameter, 140 nm shell thickness; see Supporting Information Figure S1) were dyed with RITC (red), and fluorescent core–shell silica spheres (1.5  $\mu$ m diameter) were FITC dyed (green). The aqueous sample contained a salt (NaCl) concentration of 4.5 mM, and the electric field strength was 12.5 V/mm. The scale bars denote 5  $\mu$ m in image a and 10  $\mu$ m in images b and c.

Herein, we show experimentally and theoretically that electric fields can be exploited as a new route for inducing a lock-and-key type of interaction between complementary-shaped (convex and concave) particles (polarizable bowls and spheres). The electric field is therefore an alternative to the addition of depletants. Preliminary results in this direction were already presented in ref 3. A powerful advantage is that the interaction energy can now be tuned *in situ* by external control and without the need to alter the composition of the system. Moreover, we show that the force balance can be adjusted such that even irreversibly bound composites can be generated. In this way, electric fields not only result in directed self-assembly of anisotropic particles but actually also form a means to synthesize new types of complex-shaped particles, as we will show.

## EXPERIMENTAL SECTION

**Materials.** Dimethyldiethoxysilane (DMDES, 97.0%), tetraethoxysilane (TES, 98.0%), 3-(aminopropyl)triethoxysilane (APS, 99%), rhodamine B isothiocyanate (RITC), poly(vinylpyrrolidone) (PVP; MW, 58,000 and 40,000 g/mol), styrene, deuterium oxide (D<sub>2</sub>O), fluoresceine isothiocyanate (FITC), and ammonia (25 wt % NH<sub>3</sub>) were purchased from Sigma-Aldrich. Pyromethene-567 was obtained from Exciton, ethanol (96%, 100%) was from Interchema, and PVP

(MW, 360,000 g/mol) and 2,2'-azobis(2-methylpropionitrile) (AIBN) were from Fluka. All chemicals were used as received. Demineralized water (resistivity, 18 M $\Omega$  cm) was used in all reactions and also for cleaning of glassware.

**Particle Synthesis and Characterization.** See the Supporting Information (SI).

**Sample Preparation.** Mixtures of spheres (silica or polystyrene (PS)) and bowls were prepared both in water and in D<sub>2</sub>O; see Table 1. These mixtures were obtained by combining the stock dispersions (see SI) and adding a small amount of a 33 mM NaCl stock solution and optionally D<sub>2</sub>O. Samples were homogenized using a vortex mixer (IKA minishaker MS2) at 2500 rpm for a few seconds, after which the sample cells (see later text) were filled.

**Sample Cell Preparation.** Sample cells for electric-field-induced self-assembly were constructed from borosilicate glass capillaries (VitroCom, 0.2  $\times$  2  $\times$  50 mm<sup>3</sup>) mounted on a glass cover slide (Thermo Scientific) using Scotch tape. Two electrode wires (T2 thermocouple alloy wire, Goodfellow, diameter 0.05 mm) were spanned along the inside (long axis) of the capillaries such that they were spaced 2 mm apart; see Figure 1. Filled capillaries were sealed using either candle wax or UV glue (Norland optical adhesive no. 68).

**Viscosity Step-Gradient Centrifugation.** After SA in an electric field, the different particle species (bowls, spheres, and composite particles) were separated by viscosity step-gradient centrifugation. To this end, capillaries were opened by scraping off the wax, and the

bowl/sphere mixtures were recollected from the capillary using a strong air flow.

Viscosity gradients were built as in ref 47 from aqueous PVP (MW = 40,000 g/mol) solutions of various concentrations: 5.8, 8.8, 11.8, 14.8, 18.7, 22.8, and 27.0% (w/w). Centrifuge tubes (Ultra-Clear Tubes, Beckman-Coulter, 1.5 mL) were filled with consecutive layers (275  $\mu$ L) of PVP solution, starting from the highest concentration. The sample to be separated (about 40  $\mu$ L, originating from six electric sample cells) was premixed with 120  $\mu$ L of 5.8% (w/w) PVP solution and placed on top of the step gradient. The tube was centrifuged for 25 min at 82 g (Hettich Rotina centrifuge) after which the separate bands were collected by piercing the wall of the tube using a syringe.

**Confocal Microscopy.** Electric-field-induced SA of mixtures of bowls and spheres in electric sample cells were imaged using a Leica SP2 inverted confocal microscope fitted with a Plan Apo 63 $\times$  (NA = 1.4) Leica confocal oil immersion objective. Each sample cell was placed on the sample stage with the capillary facing downward, and the objective placed against the capillary with a drop of Leica type F immersion oil. The excitation laser lines used were 488 nm (blue) for the FITC-labeled silica spheres and the pyromethene-dyed polystyrene spheres and 543 nm (green) for the RITC-labeled bowls. These laser lines were selected by acousto-optical filters (AOTFs) from the lines of an ArKr laser and a GrNe laser. The fluorescent signals were collected by photomultiplier tube (PMT) detectors in the ranges 500–535 nm (for the emission signal of FITC and pyromethene dye) and 555–620 nm (for the emission signal of RITC dye) in sequential scanning mode between lines, and at a scanning speed of 800 Hz. The pinhole size was 114.6  $\mu$ m (Airy disk). Typical images had a resolution of 512  $\times$  512 pixels and a typical pixel size of 40–100 nm.

A HP 33220A 15 MHz function/arbitrary waveform generator provided sinusoidal electric fields (1 MHz, with typically a 5 V peak-to-peak voltage). A Krohn-Hite 7602 M wideband amplifier was used for amplification of the signal to 25–40 V.

## RESULTS AND DISCUSSION

### Electric-Field-Induced Lock-and-Key Interactions.

In this work we introduce a novel route, based on electric fields rather than depletants, to induce site-specific lock-and-key interactions between colloids. To this end, aqueous mixtures of shape-complementary particles (bowls and spheres) were prepared, often containing a few millimolar of added NaCl. The exact composition of the various samples is given in Table 1. The bowl-shaped particles were made by buckling of hollow, elastic microcapsules.<sup>37,38</sup> Scanning electron microscopy images of both particle species are shown in Figure 1a. We note that the elastic bowls collapsed upon drying but have a well-defined bowl shape in solution, as can be inferred from the confocal images. The bowl-shaped particles had a diameter of 2.6  $\mu$ m and a shell thickness of 140 nm, as determined with static light scattering (SLS) and atomic force microscopy (AFM), respectively (Figure S1). The 1.48  $\mu$ m diameter of the silica particles (SLS; Figure S1) was chosen such that these spheres fitted inside the bowl-shaped cavity. An alternating electric field ( $\sim$ 1 MHz, typically 10–20 V/mm) was applied in a sample cell as shown in Figure 1a. On account of the high frequency of this alternating electric field, which is much higher than the relaxation rate of a double layer, the dominant polarization contribution stems from the particles rather than from the ionic double layers.<sup>3</sup> As reported in literature,<sup>26</sup> spheres line up in such a field to form strings since the induced polarizations prefer a head-to-toe arrangement, such as with dipoles. Bowl-shaped particles attain an orientation with the symmetry axis perpendicular to the field and form strings in which the individual particles face alternating directions (see Figure 1b and ref 3). Besides, we found that at high volume fractions

bowls stacked in the direction perpendicular to the field (Figure 1b) as well.

In mixtures of bowls and silica spheres dispersed in water and exposed to an electric field, we observed the formation of strings generally consisting of both species combined. These bowls and spheres do not phase separate since they have similar dipole moments; see our calculation in the SI. The applied field strength was low enough to allow for some particle displacements, resulting in spheres that were captured by the bowls. The majority of the bowls were typically filled with a sphere after about 30 minutes, as depicted in Figure 1c. Directly after switching off the electric field completely, the captured silica spheres were released and the individual particles performed Brownian motion again (see SI Movie S1). This also highlights directly the additional advantage of the current study as the lock-and-key interactions are now switchable by external conditions, even on millisecond time scales. This is in contrast to the conventional method based on depletants, where the interaction can only be tuned by changing the sample composition (i.e., depletant concentration) or by using temperature-tunable polymers.<sup>40</sup> Typically, when gradually reducing the electric field, filled bowls were initially aligned in strings ( $\sim$ 20 V/mm); the strings of filled bowls then broke up ( $\sim$ 10 V/mm) after which composites disassembled and bowls were no longer aligned ( $\sim$ 5 V/mm). Interestingly, a small fraction of composite particles remained intact, despite the fact that no salt was added, a point we will come back to later. Also note that the method can be generalized to other materials, provided that the zero frequency dielectric constant mismatch between colloids and solvents is sufficiently large for appreciable dipolar interactions to occur. We demonstrated this by using polystyrene spheres (1.5  $\mu$ m in diameter) instead of silica spheres (see Figure S2). The composition of this sample (PS-w4.5) is given in Table 1.

**Self-Assembly Mechanism.** To gain more insights into the previously described electric-field-induced lock-and-key interactions, we investigated the interactions of polarizable colloidal particles subject to an external electric field  $\mathbf{E} = |\mathbf{E}|\hat{e}$ , where  $\hat{e}$  denotes the direction of the field. The symmetry of a sphere renders its potential energy in an external field independent of the orientation of the field. However, the potential energy between a single bowl of orientation  $\hat{\omega}$  in an external electric field is given by<sup>35</sup>

$$U_{BE}^{dip}(\hat{\omega}, \hat{e}) = -\frac{1}{2}(\alpha_{\parallel} - \alpha_{\perp})|\mathbf{E}|^2(\hat{\omega} \cdot \hat{e})^2 + \text{const} \quad (1)$$

with the angle  $\arccos(\hat{\omega} \cdot \hat{e})$  between  $\hat{\omega}$  and the electric field direction  $\hat{e}$ . Here,  $\alpha_{\parallel}$  and  $\alpha_{\perp}$  denote the two independent components of the diagonalized polarizability tensor of the bowl, corresponding to an orientation parallel ( $\hat{\omega} \parallel \hat{e}$ ) or perpendicular ( $\hat{\omega} \perp \hat{e}$ ) to the external field.

For the experiments carried out, we find that  $(\alpha_{\parallel} - \alpha_{\perp})|\mathbf{E}|^2/2 \approx 7.3 k_B T$  for  $E = 20$  V/mm (and for dielectric constants,  $\epsilon_{\text{water}} = 80$ ,<sup>39</sup>  $\epsilon_{\text{bowl}} = 3.5$  (estimated, based on  $\epsilon_{\text{silica}} = 3.8$ <sup>39</sup>), and diameters,  $D_{\text{bowl,inner}} = 2.60$   $\mu$ m,  $D_{\text{bowl,outer}} = 2.88$   $\mu$ m) as a typical interaction energy between the bowl and the field. Here we model the bowl as a hemispherical sheet of dipoles. From these values it is apparent that a single bowl has a strong tendency to orient its symmetry axis perpendicular to the external field ( $\hat{\omega} \perp \hat{e}$ ). Thus, similar to the result of induced polarizations of other anisotropic shapes such as the spheres with partial gold coatings in ref 41, we find that the bowls align parallel with the

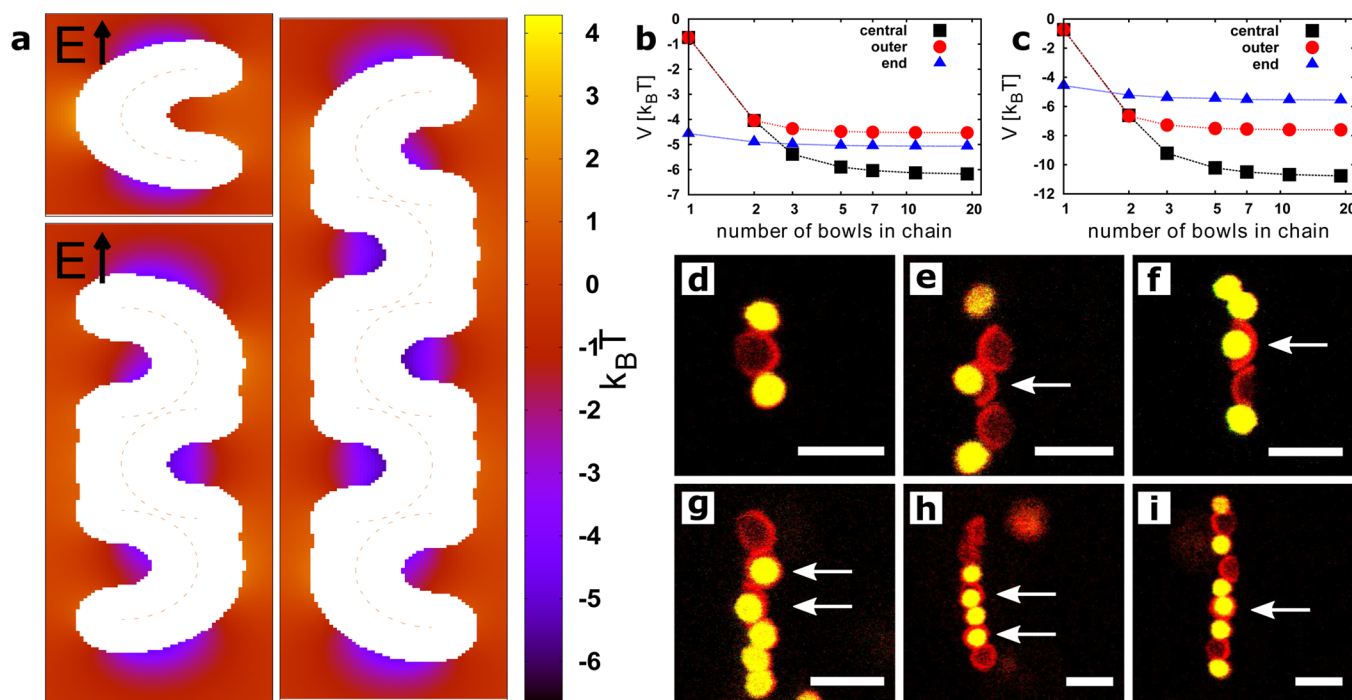


**Figure 2.** Chain length dependence of the potential energy minimum, affecting the chain configuration. (a) Field-induced “dipolar” interaction energy landscape for a sphere in the vicinity of a chain of one, three, or five aligned bowls. The (alternating) electric-field strength is 20 V/mm and acts along the direction indicated by the arrow. The white area denotes the region that is excluded for the center-of-mass position of the sphere. The color look-up table linking interaction energy to a color is shown to the right. (b) Depth of the potential well for a sphere that is added to a chain of alternating bowls under the influence of an electric field (20 V/mm), as a function of the number of bowls in the chain. The three graphs correspond to three possible positions for the sphere to be added to the chain: in a centrally located bowl, in a bowl at the end of the chain, or to the end of the chain of bowls. For a chain of three bowls or more, the potential energy minimum is deepest for a location inside a centrally located bowl. (c) Similar graphs as in panel b, but for the addition of a sphere to a chain of  $N$  bowls already filled with  $(N - 1)$  spheres. The energy minima are deeper than in panel b; i.e., the capturing of spheres promotes the capturing of additional spheres in the chain. (d–i) Confocal micrographs of strings of increasing chain length, composed of bowls and spheres. The backbone consisted of three (d), four (e), five (f), six (g), seven (h), and nine (i) particles, and filled bowls are indicated by the arrows. Note that the other spheres are part of a chain but not inside a bowl, although some bleeding-through of the red channel is visible along the edge of some spheres. Bowls (2.6  $\mu\text{m}$  diameter, 140 nm shell thickness) were dyed with RITC (red), and polystyrene spheres (1.5  $\mu\text{m}$  diameter) were dyed with pyromethene throughout (yellow). The sample was prepared in (57% (v/v))  $\text{D}_2\text{O}$  with  $[\text{NaCl}] = 3.8$  mM. Here,  $E = 15$  V/mm. The scale bars denote 5  $\mu\text{m}$ .

field (i.e., with their symmetry axes perpendicular to the field) and form chains/strings in the field direction.

We now turn our attention to the field-induced “dipolar” interaction between a silica sphere ( $\epsilon_{\text{sphere}} \approx \epsilon_{\text{bowl}} = 3.5$  and  $D_{\text{sphere}} = 1.48$   $\mu\text{m}$ ) and one, three, and five aligned bowls. Approximating the induced dipole density inside the particles as homogeneous, the dipolar interaction between two particles  $i$  and  $j$  with volumes  $V_i$  and  $V_j$  is given by

$$U_{ij}^{\text{dip}}(\mathbf{r}_{ij}, \hat{\epsilon}) = \frac{1}{V_i V_j} \int_{V_i} \int_{V_j} d\mathbf{r}_1 d\mathbf{r}_2 u(\mathbf{r}_{ij} + \mathbf{r}_1 - \mathbf{r}_2, \hat{\epsilon}) \quad (2)$$

where  $\mathbf{r}_{ij}$  denotes the distance between the respective centers of the particles and where the integrations are over the volumes of both particles. Here the potential between two aligned point dipoles at separation  $r$  is given by

$$u(\mathbf{r}, \hat{\epsilon}) = \frac{p_i p_j}{4\pi\epsilon_{\text{water}}\epsilon_0} \frac{1 - 3(\hat{\epsilon} \cdot \mathbf{r}/|\mathbf{r}|)^2}{|\mathbf{r}|^3} \quad (3)$$

where  $\epsilon_0$  and  $\epsilon_{\text{water}}$  are the dielectric constants of vacuum and the solvent, in this case either pure water or a mixture of  $\text{H}_2\text{O}$  and  $\text{D}_2\text{O}$ . Using the Clausius–Mossotti equation, we estimate the dipole moments  $p_i$  and  $p_j$  of the point dipoles in both kinds of particles as

$$\mathbf{p}_i = 3\epsilon_{\text{water}}\epsilon_0 V_i \frac{\epsilon_i - \epsilon_{\text{water}}}{\epsilon_i + 2\epsilon_{\text{water}}} \mathbf{E} \quad (4)$$

On the basis of eqs 2–4, we calculate the field-induced dipolar interaction of a single sphere and one, three, and five aligned bowls as a function of the position of the sphere with respect to the (string of) bowls and present the interaction energy landscape in Figure 2a. For a single bowl, a location next to the bowl (along the field direction) has the deepest potential energy well and is therefore favorable for the sphere. For a chain composed out of three bowls, a location inside the bowls becomes energetically favorable, with the largest potential energy minimum inside the centrally located bowl. The potential energy minima as a function of chain length are studied further in Figure 2b,c, which display the dipolar interaction energy for a sphere positioned at different locations along the chain: inside a bowl in the center of the chain, inside a bowl at the outer end of the chain, and attached to the outer end of the chain. Figure 2b concerns a chain of “empty” bowls. It is clear that, for a chain of at least three bowls, the potential energy minimum is deepest for the bowl in the middle of the chain. Figure 2c concerns the addition of a sphere to a chain of  $N$  bowls filled with  $(N - 1)$  spheres. The potential energy minima are even deeper in this case, as compared to the case of an empty chain of bowls. Hence, the capturing of spheres

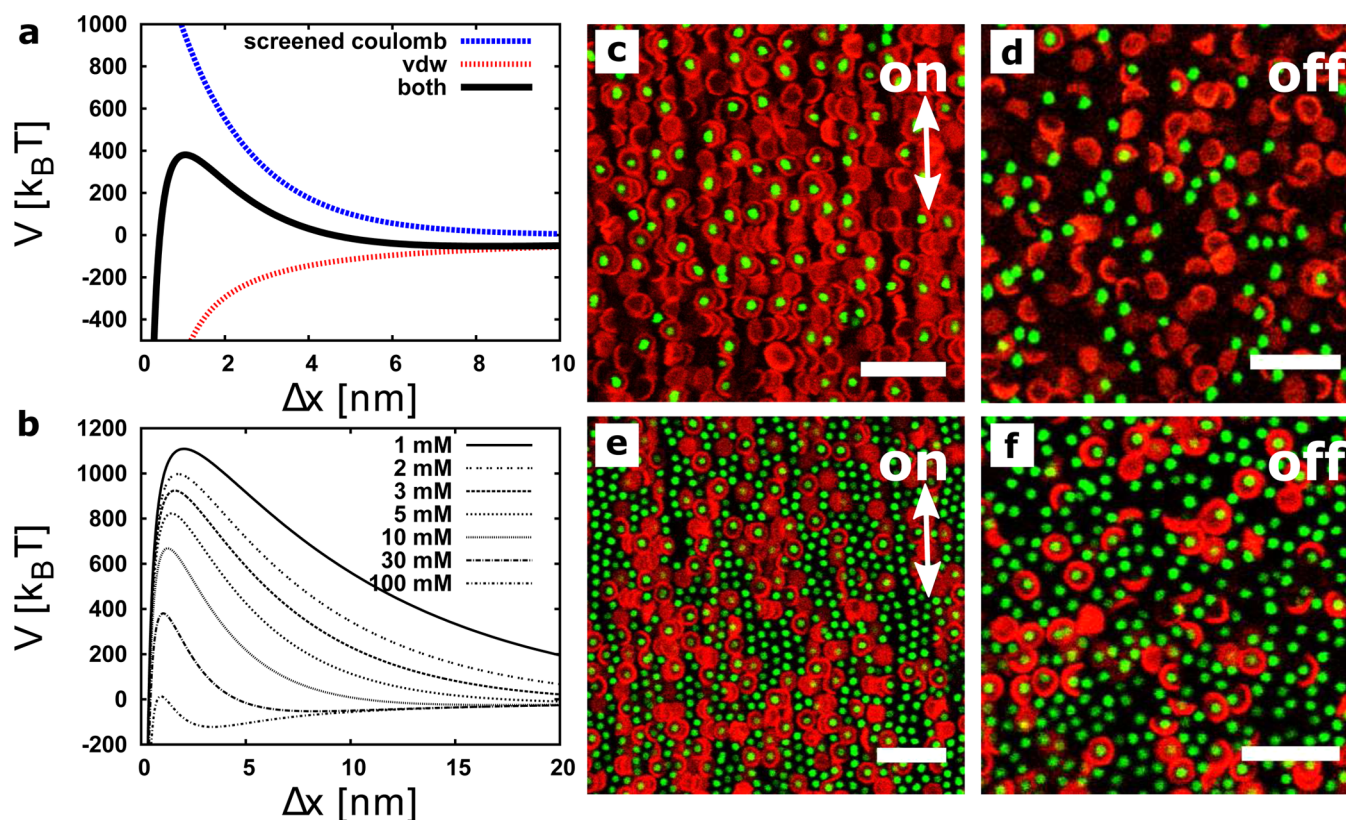


**Figure 3.** Creation of irreversible “sphere-in-bowl” composite particles allowed by van der Waals attractions. (a) van der Waals (red), screened Coulomb (blue), and combined (black) potential as a function of the surface-to-surface distance of a bowl and a sphere on the symmetry axis of the bowl, for  $\rho_{\text{salt}} = 30$  mM. The parameters used in the calculation are  $\epsilon_{\text{water}} = 80$ ,  $\epsilon_{\text{sphere}} \approx \epsilon_{\text{bowl}} = 3.5$ ,  $D_{\text{sphere}} = 1.48 \mu\text{m}$ ,  $D_{\text{bowl,inner}} = 2.60 \mu\text{m}$ , and  $D_{\text{bowl,outer}} = 2.88 \mu\text{m}$ . (b) Similar potentials as in panel a, but for various salt concentrations. (c, d) Reversible lock-and-key interactions between bowls and spheres observed when the number of bowls exceeded the number of spheres. The aqueous sample contained a salt (NaCl) concentration of 4.5 mM, and the electric field (12.5 V/mm) was applied for a period of  $\sim 5.5$  h (c) after which it was switched off (d). (e, f) Irreversibly bound composite particles of spheres in bowls were observed when the number of spheres exceeded the number of bowls. The salt (NaCl) concentration in the aqueous medium was 8.2 mM. The electric field (20 V/mm) was applied for 1 h (e) after which it was switched off (f). Bowls (2.6  $\mu\text{m}$  diameter, 140 nm shell thickness) were dyed with RITC (red), and fluorescent core–shell silica spheres (1.5  $\mu\text{m}$  diameter) were FITC dyed (green). The scale bars denote 10  $\mu\text{m}$ .

promotes the capturing of additional spheres in the chain. Note that the potential energy minimum is still deepest for a location inside a centrally located bowl. However, compared to the case of an empty chain of bowls, a location inside a bowl at the outer end of a chain now becomes energetically preferable over a location at the end of the chain. This further enhances the capturing of spheres for chains of bowls which are already partially filled.

These theoretical predictions imply that longer chains are required for successful electric-field-induced SA. To validate this theoretical result, experiments were performed with a partially density-matched dispersion, such that the particles were more homogeneously spread throughout the volume of the sample cell, resulting in shorter chains. To this end, polystyrene spheres were used in combination with the bowls and were density-matched in the solvent  $\text{D}_2\text{O}$  (sample PS-d3.8, Table 1). Representative confocal micrographs are shown in Figure 2d–i. Experimentally, the shortest observed chains consisted of three particles in the backbone. Within this geometry, only one out of the six monitored chains contained a bowl with a captured sphere. This is in strong contrast to significantly larger chains, consisting of at least seven particles in the backbone. Note that the backbones predominantly consist of bowls but that spheres are taken up in the backbones

of some chains as well. Here, the five studied chains all contained at least one composite particle. This scenario was also confirmed while recording a time series (see Movie S2). During the experimentally considered time scale, a backbone of three particles was stable in the sense that it was not observed to collapse into a backbone of two particles with one particle filled. However, a sphere was captured by an approaching bowl that was part of a backbone consisting of initially four particles. Despite the limited statistics of these observations, these experimental findings are consistent with the theoretical calculations on the field-induced interactions, which indicated that the self-assembly process requires sufficiently long chains to induce lock-and-key interactions (i.e., at least three or four particles in the backbone) for the cases studied in this work.

**Irreversibly Bound Composite Particles.** Although the induced dipolar interactions (eqs 2–4) describe the capture probability of spheres in terms of the energy landscape of Figure 2 on the micrometer length scale, it cannot account for the irreversible binding between bowls and spheres that is also observed. We therefore extend our theoretical analysis to also account for van der Waals attractions due to the dielectric constant mismatch between particles and solvent, and for screened Coulomb repulsions that originate from the electrostatic repulsion between the like-charged particle surfaces and

double layer overlap (Figure 3a). While the dipolar interaction plays a dominant role for distances between the particles larger than  $\sim 10$  nm, we find that once the surfaces of two particles approach each other closely (in the range of several nanometers), it is quickly exceeded by van der Waals attractions and Coulomb repulsions of the surface charges. Within the Hamaker–de Boer description, we write the van der Waals interaction potential between a sphere (radius  $R_S$ ) and a bowl as<sup>42,43</sup>

$$U_{BS}^{vdW}(\mathbf{r}_{SB}) = -\frac{A_{SB}}{\pi} \int_{V_B} d\mathbf{r}' \frac{4R_S^3}{3(|\mathbf{r}_{SB} - \mathbf{r}'| - R_S)^3 (|\mathbf{r}_{SB} - \mathbf{r}'| + R_S)^3} \quad (5)$$

where  $A_{SB}$  is the Hamaker constant and  $\mathbf{r}_{SB}$  the distance between the centers of the sphere and the bowl and the integration is over the volume of the bowl. Note that eq 5 reduces to the familiar  $|r_{SB}|^{-6}$  scaling for large bowl–sphere separations, which gets modified at smaller separations by the finite volume of the sphere and the bowl. One could consider a further simplification within, e.g., the Derjaguin approximation, but here we opted for the full numerical evaluation of the integral in eq 5. Here we did not take retardation effects into account.

We model the interaction of the surface charges of the particles by integrating the screened Coulomb interactions (which account for both osmotic and electrostatic forces) between the (assumed constant) surface charge densities  $\sigma_S$  and  $\sigma_B$  over both surfaces  $S_S$  and  $S_B$ ,

$$U_{BS}^{Coul}(\mathbf{r}_{SB}) = \frac{\sigma_S \sigma_B}{4\pi \epsilon_{water} \epsilon_0} \int_{S_S} d\mathbf{r}_1 \int_{S_B} d\mathbf{r}_2 \frac{e^{-\kappa|\mathbf{r}_{SB} + \mathbf{r}_1 - \mathbf{r}_2|}}{|\mathbf{r}_{SB} + \mathbf{r}_1 - \mathbf{r}_2|} \quad (6)$$

where the inverse screening length is given by  $\kappa = \sqrt{8\pi\lambda_B\rho_{salt}}$ , with  $\lambda_B$  the Bjerrum length and  $\rho_{salt}$  the salt concentration in the solvent.<sup>43,44</sup> The surface charges of the particles are estimated by the  $\zeta$  potential  $\phi_S$  of the sphere and  $\phi_B$  of the bowl. The experimentally determined  $\zeta$  potentials were  $-58 \pm 7$  mV for the silica spheres and  $-56 \pm 6$  mV for the polystyrene spheres and  $-32 \pm 5$  mV for the bowls (see SI, characterization section). We used these experimental  $\zeta$  potentials to match the charge density on the surface to that of a particle near a planar surface by<sup>44</sup>

$$\sigma_{S,B} = \phi_{S,B} \kappa \epsilon_0 \epsilon \quad (7)$$

In Figure 3a we show the van der Waals and Coulombic potential separately as well as combined, as a function of the surface-to-surface distance ( $\Delta x$ ) of a bowl and a sphere on the symmetry axis of the bowl, for  $\rho_{salt} = 30$  mM, revealing a picture that is consistent with the well-known DLVO theory: a deep primary minimum at  $\Delta x \leq 1$  nm and a much more shallow secondary minimum at  $\Delta x \approx 10$  nm, separated by a barrier of  $400 kT$ . For these parameters, one does not expect irreversible binding since the barrier would prevent any approach below the 1 nm distance. In Figure 3b the sum of van der Waals and screened Coulomb interactions is plotted in the same regime but now for a variety of salt concentrations  $\rho_{salt}$ . The barrier increases with lowering  $\rho_{salt}$ , as expected, and decreases at higher  $\rho_{salt}$  to essentially vanish at  $\rho_{salt} = 100$  mM. We could thus expect irreversible binding in the primary minimum at high enough salt concentrations.

We found experimentally that, in the case of a surplus of bowls, a small fraction of composite particles remained irreversibly bound after switching off the electric field (Figure 3c,d, taken of sample SiO<sub>2</sub>-w4.5-2). This fraction did not significantly increase upon addition of salt (NaCl; maximum concentration investigated, 30 mM). In the case of a surplus of spheres, however, adding salt was found to shift the SA from reversible to irreversible binding. In the absence of salt, the majority of the composite particles were reversibly bound, similar to the behavior for an excess of bowls. At a salt concentration of 4.5 mM (sample SiO<sub>2</sub>-w4.5-1) or 8.3 mM (sample SiO<sub>2</sub>-w8.3) (Figure 3e,f), most composite particles were irreversibly bound (see SI Movie S3). These experiments are consistent with the theoretical prediction that binding can become irreversible at high enough salt concentrations. Unfortunately the strong dependency on the salt concentration with respect to the mixing ratio of bowls and spheres could not be clarified from our theory. Possibly, this observation is caused by many-body interactions that we do not currently understand. When DLVO stability barriers approach nanometer distances, surface roughness<sup>45</sup> and charge patchiness<sup>46</sup> can induce aggregation but one still needs a many-body approach to explain the dependence in irreversible aggregation on the sphere-to-bowl mixing ratio. Notwithstanding this, the ability to tune the reversible and irreversible behavior directly points to an important additional feature of our methodology: one can now also use this new self-assembly method for synthesis of colloids of complex shapes and mixed composition.

**Isolating Composite Particles.** The irreversible binding of spheres inside bowls allowed us to harvest the composite particles from the mixture of spheres, bowls, and composite colloids in sample SiO<sub>2</sub>-w8.3 (see Table 1). The composite colloids were initially formed during 1 h in an electric field of 20 V/mm (see Figure 3f). A viscosity step gradient<sup>47</sup> was used to separate the three types of particle species over three distinct bands (Figure 4a). Viscosity step-gradient centrifugation as opposed to density-gradient centrifugation exploits the fact that a gradient in viscosity reduces the settling velocity of a particle by a larger amount than a density gradient does. For example, a simple calculation in ref 47 states that, for a particle with a specific density of 5 g/mL, the settling velocity decreases only by 25% as the medium's density increases from 1 to 2 g/mL, whereas a viscosity increase induced by going from 10% PVP to 30% PVP nearly reduces the settling velocity by 87.3%. Therefore, the viscosity gradient is better suited to separate "heavy" particles. In the case of Qiu and Mao the heavy particles are gold nanoparticles (i.e., particles of high specific density), whereas our particles are heavy due to their colloidal size.

After recollecting the bands, confocal microscopy confirmed that each band contained a different type of particle. The top band contained only bowls, followed by the middle band that contained the composite particles and the lower band that contained single spheres (Figure 4b–f). This separation was performed about an hour after self-assembly, further proving the long-term stability of the composite particles.

## CONCLUSIONS

In summary, we have shown that external electric fields can be used in a novel route to induce lock-and-key interactions in a binary system of convex and concave particles. The additional advantage, with respect to depletion interactions, is that these interactions are reversible and can be controlled on millisecond

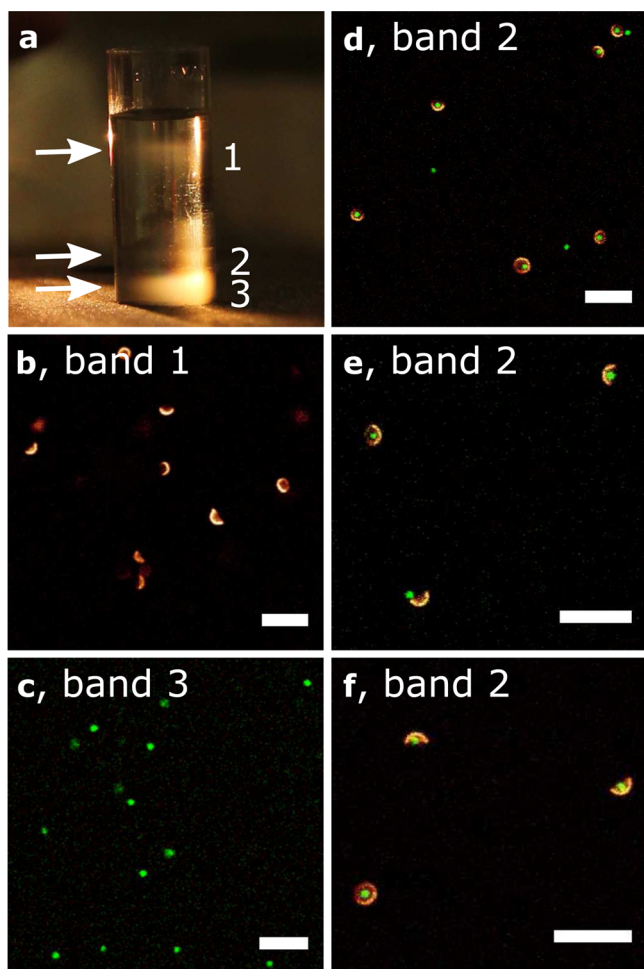


**Figure 4.** Collecting composite particles using a stepwise viscosity gradient combined with centrifugation. (a) Separation of bowls (band 1), composite particles (band 2), and spheres (band 3) in a PVP viscosity step gradient. (b–f) Confocal micrographs of the bowls in band 1 (b), spheres in band 3 (c), and composite particles in band 2 (d–f). Bowls (2.6  $\mu\text{m}$  diameter, 140 nm shell thickness) were dyed with RITC (red), and silica spheres (1.5  $\mu\text{m}$  diameter) were FITC dyed (green). The scale bars denote 10  $\mu\text{m}$ .

time scales. In this way, we have prepared reversibly bound composite particles consisting of shape-complementary bowls and spheres. These experiments can be extended to many different materials, and as a proof of principle we already used both silica and polystyrene spheres. Through calculations of the relevant interparticle interactions (using the materials parameters studied in this work, i.e., dielectric constants  $\epsilon_{\text{water}} = 80$  and  $\epsilon_{\text{sphere}} \approx \epsilon_{\text{bowl}} = 3.5$  and diameters  $D_{\text{sphere}} = 1.48 \mu\text{m}$ ,  $D_{\text{bowl,inner}} = 2.60 \mu\text{m}$ , and  $D_{\text{bowl,outer}} = 2.88 \mu\text{m}$ ), we have shown that, in an electric field, a potential minimum exists for the spheres inside the bowls, provided the backbone of the chain of colloids contains at least three particles (bowls, or spheres taken up in the chain). The force balance of the bowls and spheres was also tuned (by adding salt and by varying the ratio of the number of convex and concave particles), such that the majority of composite particles remained irreversibly bound even after the field was turned off. These composite particles were purified from the single components by simply using a viscosity step gradient combined with centrifugation. Although the scale of the current experiment was small, there are no fundamental obstacles to scaling it up. We thereby have shown

that this mechanism provides a new route not only for self-assembly but also for synthesis of colloids of complex shapes. A just accepted paper by Tatsuno et al.<sup>48</sup> shows that size selectivity based on convex and concave shapes can also be utilized in materials sensing, specifically the sensing of viruses.

Our method can be further extended and generalized in the sense that one does not need to rely on van der Waals attractions. This could be achieved by coating one of the two components of our convex and concave particles with two different layers of polyelectrolytes: the first layer of opposite charge and the second layer of the same charge as the charge of the other component. Bringing the particles together with electric fields will now also expose the lower layer of oppositely charged polyelectrolyte to the other component. The particles are then bound by electrostatic interactions instead of van der Waals interactions. This method, already used in ref 26, will therefore make our attachment strategy more easily controllable.

Finally, we stress that this SA method can also be extended to particles with flat facets (hence flat–flat combinations). Although the concave–convex combination in this study is probably most efficient, making a spherical shape flat<sup>18</sup> will still reduce the electric field strength required for SA when compared to sphere–sphere or sphere–flat combinations of particles. The general potential of strengthening interparticle interactions in self-assembly studies with flattened particles was already reported in refs 5 and 49.

## ■ ASSOCIATED CONTENT

### 📄 Supporting Information

The Supporting Information is available free of charge on the ACS Publications website at DOI: 10.1021/acs.chemmater.5b04152.

Additional details on the experimental methods, additional Figures S1 and S2, and an additional calculation (PDF)

Movie 1 showing bowls and silica spheres in  $\text{H}_2\text{O}$  in an electric field (AVI)

Movie 2 showing bowls and polystyrene spheres in  $\text{D}_2\text{O}$  in an electric field (ZIP)

Movie 3 showing bowls and a surplus of silica spheres in  $\text{H}_2\text{O}$  (ZIP)

## ■ AUTHOR INFORMATION

### Corresponding Authors

\*(M.K.) E-mail: [M.Kamp@uu.nl](mailto:M.Kamp@uu.nl).

\*(A.v.B.) E-mail: [A.vanBlaaderen@uu.nl](mailto:A.vanBlaaderen@uu.nl).

### Author Contributions

<sup>†</sup>M.K., N.A.E., and T.T. contributed equally to this work. A.v.B. and A.I. initiated the experimental part of the project, and R.v.R. and M.D., the theoretical part of the project. M.K. and N.A.E. performed all experiments in close collaboration and under the supervision of A.v.B.. T.T. performed the theoretical studies under the supervision of M.D. and R.v.R.. The manuscript was co-written by M.K., N.A.E., T.T., M.D., R.v.R., and A.v.B.. All authors analyzed and discussed the results.

### Notes

The authors declare no competing financial interest.

## ACKNOWLEDGMENTS

We kindly thank Esther Vermolen and Bo Peng for providing the SiO<sub>2</sub> and PS spheres, respectively. Judith Wijnhoven is acknowledged for the Scanning Electron Micrographs in Figure 1. M.K. received financial support from the Netherlands Organisation for Scientific Research (NWO) through an ECHO grant (project 700.58.025). Moreover, funding was received from the European Research Council under the European Unions Seventh Framework Programme (FP/2007-2013)/ERC Grant Agreement no. 291667. N.A.E. is supported by the Industrial Partnership Programme (IPP) Innovative Physics for Oil and Gas (iPOG) of the Stichting voor Fundamenteel Onderzoek der Materie (FOM), which is supported financially by the Netherlands Organisation for Scientific Research (NWO). The IPP iPOG is cofinanced by Stichting Shell Research. This work is also part of the D-ITP consortium and the DFG/FOM program SFB-TR6 (project B8); both these NWO programs are funded by the Dutch Ministry of Education, Culture and Science (OCW).

## REFERENCES

- (1) Glotzer, S. C.; Solomon, M. J. Anisotropy of Building Blocks and their Assembly into Complex Structures. *Nat. Mater.* **2007**, *6*, 557–562.
- (2) Yoon, J.; Lee, K. J.; Lahann, J. Multifunctional Polymer Particles with Distinct Compartments. *J. Mater. Chem.* **2011**, *21*, 8502–8510.
- (3) van Blaaderen, A.; Dijkstra, M.; van Roij, R.; Imhof, A.; Kamp, M.; Kwaadgras, B. W.; Vissers, T.; Liu, B. Manipulating the Self Assembly of Colloids in Electric Fields. *Eur. Phys. J.: Spec. Top.* **2013**, *222*, 2895–2909.
- (4) Zoldesi, C. I.; Imhof, A. Synthesis of Monodisperse Colloidal Spheres, Capsules, and Microballoons by Emulsion Templating. *Adv. Mater.* **2005**, *17*, 924–928.
- (5) Ramirez, L. M.; Michaelis, C. A.; Rosado, J. E.; Pabón, E. K.; Colby, R. H.; Velegol, D. Polloidal Chains from Self-Assembly of Flattened Particles. *Langmuir* **2013**, *29*, 10340–10345.
- (6) Kuijk, A.; van Blaaderen, A.; Imhof, A. Synthesis of Monodisperse, Rodlike Silica Colloids with Tunable Aspect Ratio. *J. Am. Chem. Soc.* **2011**, *133*, 2346–2349.
- (7) Hijnen, N.; Clegg, P. S. Simple Synthesis of Versatile Akaganeite-Silica Core-Shell Rods. *Chem. Mater.* **2012**, *24*, 3449–3457.
- (8) Rossi, L.; Sacanna, S.; Irvine, W. T. M.; Chaikin, P. M.; Pine, D. J.; Philipse, A. P. Cubic Crystals from Cubic Colloids. *Soft Matter* **2011**, *7*, 4139–4142.
- (9) Mohraz, A.; Solomon, M. J. Direct Visualization of Colloidal Rod Assembly by Confocal Microscopy. *Langmuir* **2005**, *21*, 5298–5306.
- (10) Lee, S. H.; Song, Y.; Hosein, I. D.; Liddell, C. M. Magnetically Responsive and Hollow Colloids from Nonspherical Core-Shell Particles of Peanut-like Shape. *J. Mater. Chem.* **2009**, *19*, 350–355.
- (11) Wijnhoven, J. E. G. J. Seeded Growth of Monodisperse Gibbsite Platelets to Adjustable Sizes. *J. Colloid Interface Sci.* **2005**, *292*, 403–409.
- (12) Kraft, D. J.; Vlug, W. S.; van Kats, C. M.; van Blaaderen, A.; Imhof, A.; Kegel, W. K. Self-Assembly of Colloids with Liquid Protrusions. *J. Am. Chem. Soc.* **2009**, *131*, 1182–1186.
- (13) Peng, B.; van Blaaderen, A.; Imhof, A. Direct Observation of the Formation of Liquid Protrusions on Polymer Colloids and Their Coalescence. *ACS Appl. Mater. Interfaces* **2013**, *5*, 4277–4284.
- (14) Perro, A.; Duguet, E.; Lambert, O.; Taveau, J.-C.; Bourgeat-Lami, E.; Ravaine, S. Chemical Synthetic Route towards "Colloidal Molecules. *Angew. Chem., Int. Ed.* **2009**, *48*, 361–365.
- (15) Manoharan, V. N.; Elsesser, M. T.; Pine, D. J. Dense Packing and Symmetry in Small Clusters of Microspheres. *Science* **2003**, *301*, 483–487.
- (16) Peng, B.; Vutukuri, H. R.; van Blaaderen, A.; Imhof, A. Synthesis of Fluorescent monodisperse Non-Spherical Dumbbell-like Model Colloids. *J. Mater. Chem.* **2012**, *22*, 21893–21900.
- (17) Cheng, Z.; Luo, F.; Zhang, Z.; Ma, Y. Syntheses and Applications of Concave and Convex Colloids with Precisely Controlled Shapes. *Soft Matter* **2013**, *9*, 11392–11397.
- (18) Vutukuri, H. R.; Imhof, A.; van Blaaderen, A. Fabrication of Polyhedral Particles from Spherical Colloids and their Self-Assembly into Rotator Phases. *Angew. Chem., Int. Ed.* **2014**, *53*, 13830–13834.
- (19) Sacanna, S.; Korpics, M.; Rodriguez, K.; Colón-Meléndez, L.; Kim, S.-H.; Pine, D. J.; Yi, G.-R. Shaping Colloids for Self-Assembly. *Nat. Commun.* **2013**, *4*, 1688.
- (20) Sacanna, S.; Irvine, W. T. M.; Chaikin, P. M.; Pine, D. J. Lock and Key Colloids. *Nature* **2010**, *464*, 575–578.
- (21) Colón-Meléndez, L.; Beltran-Villegas, D. J.; van Anders, G.; Liu, J.; Spellings, M.; Sacanna, S.; Pine, D. J.; Glotzer, S. C.; Larson, R. G.; Solomon, M. J. Binding Kinetics of Lock and Key Colloids. *J. Chem. Phys.* **2015**, *142*, 174909.
- (22) Asakura, S.; Oosawa, F. Interaction between Particles Suspended in Solutions of Macromolecules. *J. Polym. Sci.* **1958**, *33*, 183–192.
- (23) Kuijk, A.; Troppenz, T.; Fillion, L.; Imhof, A.; van Roij, R.; Dijkstra, M.; van Blaaderen, A. Effect of External Electric Fields on the Phase Behavior of Colloidal Silica Rods. *Soft Matter* **2014**, *10*, 6249–6255.
- (24) Liu, B.; Besseling, T. H.; Hermes, M.; Demirörs, A. F.; Imhof, A.; van Blaaderen, A. Switching Plastic Crystals of Colloidal Rods with Electric Fields. *Nat. Commun.* **2014**, *5*, 3092.
- (25) Mittal, M.; Furst, E. M. Electric Field-Directed Convective Assembly of Ellipsoidal Colloidal Particles to Create Optically and Mechanically Anisotropic Thin Films. *Adv. Funct. Mater.* **2009**, *19*, 3271–3278.
- (26) Vutukuri, H. R.; Demirörs, A. F.; Peng, B.; van Oostrum, P. D. J.; Imhof, A.; van Blaaderen, A. Colloidal Analogues of Charged and Uncharged Polymer Chains with Tunable Stiffness. *Angew. Chem., Int. Ed.* **2012**, *51*, 11249–11253.
- (27) Nagao, D.; Sugimoto, M.; Okada, A.; Ishii, H.; Konno, M.; Imhof, A.; van Blaaderen, A. Directed Orientation of Asymmetric Composite Dumbbells by Electric Field Induced Assembly. *Langmuir* **2012**, *28*, 6546–6550.
- (28) Singh, J. P.; Lele, P. P.; Nettesheim, F.; Wagner, N. J.; Furst, E. M. One- and Two-Dimensional Assembly of Colloidal Ellipsoids in ac Electric Fields. *Phys. Rev. E* **2009**, *79*, 050401.
- (29) Crassous, J. J.; Mihut, A. M.; Wernersson, E.; Pfeleiderer, P.; Vermant, J.; Linse, P.; Schurtenberger, P. Field-Induced Assembly of Colloidal Ellipsoids into Well-Defined Microtubules. *Nat. Commun.* **2014**, *5*, 5516.
- (30) Erb, R. M.; Son, H. S.; Samanta, B.; Rotello, V. M.; Yellen, B. B. Magnetic Assembly of Colloidal Superstructures with Multipole Symmetry. *Nature* **2009**, *457*, 999–1002.
- (31) Ma, H.; Wen, W.; Tam, W. Y.; Sheng, P. Dielectric Electrorheological Fluids: Theory and Experiment. *Adv. Phys.* **2003**, *52*, 343–383.
- (32) Hynninen, A.-P.; Dijkstra, M. Phase Behavior of Dipolar Hard and Soft Spheres. *Phys. Rev. E* **2005**, *72*, 051402.
- (33) Hynninen, A.-P.; Dijkstra, M. Phase Diagram of Dipolar Hard and Soft Spheres: Manipulation of Colloidal Crystal Structures by an External Field. *Phys. Rev. Lett.* **2005**, *94*, 138303.
- (34) Zhang, X.; Zhang, Z. L.; Glotzer, S. C. Simulation Study of Dipole-Induced Self-Assembly of Nanocubes. *J. Phys. Chem. C* **2007**, *111*, 4132–4137.
- (35) Kwaadgras, B. W.; Verdult, M.; Dijkstra, M.; van Roij, R. Polarizability and Alignment of Dielectric Nanoparticles in an External Electric Field: Bowls, Dumbbells, and Cuboids. *J. Chem. Phys.* **2011**, *135*, 134105.
- (36) Kwaadgras, B. W.; Dijkstra, M.; van Roij, R. Communication: Bulkiness versus Anisotropy: the Optimal Shape of Polarizable Brownian Nanoparticles for Alignment in Electric Fields. *J. Chem. Phys.* **2012**, *136*, 131102.

- (37) Jose, J.; Kamp, M.; van Blaaderen, A.; Imhof, A. Unloading and Reloading Colloidal Microcapsules with Apolar Solutions by Controlled and Reversible Buckling. *Langmuir* **2014**, *30*, 2385–2393.
- (38) Elbers, N. A.; Jose, J.; Imhof, A.; van Blaaderen, A. Bulk Scale Synthesis of Monodisperse PDMS Droplets above  $3\mu\text{m}$  and their Encapsulation by Elastic Shells. *Chem. Mater.* **2015**, *27*, 1709–1719.
- (39) Depasse, J. Silica Hydrosols: Influence of the Refractive Index of the Electrolyte Solution on the Turbidity and on the Interparticle Interactions. *J. Colloid Interface Sci.* **1997**, *188*, 229–231.
- (40) Fernandes, G. E.; Beltran-Villegas, D. J.; Bevan, M. A. Interfacial Colloidal Crystallization via Tunable Hydrogel Depletants. *Langmuir* **2008**, *24*, 10776–10785.
- (41) Gangwal, S.; Pawar, A.; Kretzschmar, I.; Velev, O. D. Programmed assembly of metallodielectric patchy particles in external AC electric fields. *Soft Matter* **2010**, *6*, 1413–1418.
- (42) Hamaker, H. C. The London-van der Waals Attraction between Spherical Particles. *Physica* **1937**, *4*, 1058–1072.
- (43) Hunter, R. J. *Foundations of Colloid Science*, 2nd ed.; Oxford University Press: Oxford, U.K., 2001.
- (44) Israelachvili, J. N. *Intermolecular and Surface Forces*; Academic Press: London, U.K., 1991.
- (45) Hanus, L. H.; Hartzler, R. U.; Wagner, N. J. Electrolyte-induced aggregation of acrylic latex. 1. Dilute particle concentrations. *Langmuir* **2001**, *17*, 3136–3147.
- (46) Velegol, D.; Catana, S.; Anderson, J. L.; Garoff, S. Tangential Forces between Nontouching Colloidal Particles. *Phys. Rev. Lett.* **1999**, *83*, 1243–1246.
- (47) Qiu, P.; Mao, C. Viscosity Gradient as a Novel Mechanism for the Centrifugation-Based Separation of Nanoparticles. *Adv. Mater.* **2011**, *23*, 4880–4885.
- (48) Tatsuno, T.; Okamoto, T.; Ezaki, T.; Isobe, T.; Nakajima, A.; Matsushita, S. Metal Nanostructures Fabricated by the Difference of Interfacial Energy at a Dielectric/Metal Interface. *Bull. Chem. Soc. Jpn.* DOI: [10.1246/bcsj.20150364](https://doi.org/10.1246/bcsj.20150364) Published Online: Dec 10, 2015.
- (49) Lu, F.; Yager, K. G.; Zhang, Y.; Xin, H.; Gang, O. Superlattices Assembled through Shape-Induced Directional Binding. *Nat. Commun.* **2015**, *6*, 6912.